Special Section: Vadose Zone Modeling
Vadose Zone Journal

Leaching with Subsurface Drip Irrigation under Saline, Shallow Groundwater Conditions

Blaine Hanson,* Jan W. Hopmans, and Jirka Šimůnek

One option for coping with the high soil salinity levels caused by saline, shallow groundwater conditions along the west side of the San Joaquin Valley is to convert from sprinkler or surface irrigation methods to drip irrigation. Experiments in commercial fields revealed that subsurface drip irrigation of processing tomato (*Lycopersicon esculentum* Mill. var. *esculentum*) is highly profitable under these conditions compared with other irrigation methods. The experiments also showed that little or no field-wide leaching occurred, based on the conventional or water balance approach to estimating the leaching fraction (LF), yet soil salinity measurements showed considerable leaching around the drip lines. Actual LFs could not be calculated because LF, soil salinity, soil water content, and root density all varied with distance and depth around the drip lines. Therefore, we conducted a numerical modeling study using the HYDRUS-2D computer simulation model to evaluate leaching with drip irrigation under saline, shallow groundwater conditions for different amounts of applied water, water table depths, and irrigation water salinity, described by the electrical conductivity of the irrigation water (EC_{iw}). Results showed that LF values ranged from 7.7 to 30.9% as applied water amounts increased from 60 to 115% of the potential evapotranspiration (ET_{pot}) for the EC_{iw} = 0.3 dS m^{-1} irrigation water, even though the water balance method showed no leaching for applied water amounts equal to or smaller than ET_{pot}. The spatially varying soil wetting patterns that occur under drip irrigation caused the localized leaching, which was concentrated near the drip line.

Abbreviations: AW, applied irrigation water as a percentage of potential daily evapotranspiration; EC, electrical conductivity or salinity; ET, evapotranspiration; LF, leaching fraction.

About 400,000 ha of irrigated land along the west side of the San Joaquin Valley of California continues to be plagued by saline soil conditions caused by saline, shallow groundwater (California Department of Water Resources, 2005). Artificial subsurface drainage is not an option for controlling the salinity and waterlogging problems caused by the shallow groundwater because after more than 30 yr of research to date (2007), no economically, technically, and environmentally feasible drain water disposal methods exist. Thus, the drainage and salinity problems must be addressed by better management of irrigation water to control groundwater levels and reduce subsurface drainage, increased crop water use of shallow groundwater without yield reductions, and drainage water reuse for irrigation (Hanson and Ayars, 2002). Schoups et al. (2005) concluded that continued irrigation is not sustainable in these salt-affected areas without changing management practices.

B. Hanson and J.W. Hopmans, Dep. of Land, Air and Water Resources, Univ. of California, Davis, CA 95616; J. Šimůnek, Dep. of Environmental Sciences, Univ. of California, Riverside, CA 92521. Received 22 Mar. 2007.
*Corresponding author (brhanson@ucdavis.edu).

Vadose Zone J. 7:810–818
doi:10.2136/vzj2007.0053

© Soil Science Society of America
677 S. Segoe Rd. Madison, WI 53711 USA.
All rights reserved. No part of this periodical may be reproduced or transmitted in any form or by any means, electronic or mechanical, including photocopying, recording, or any information storage and retrieval system, without permission in writing from the publisher.

One option is to convert from furrow or sprinkle irrigation to drip irrigation. Drip irrigation can apply water both precisely and uniformly at a high irrigation frequency compared with furrow and sprinkler irrigation, thus potentially reducing subsurface drainage, providing better soil salinity control, and increasing yield. The potential is not only governed by the technology, but also by the design, installation, operation, and maintenance of drip systems. The main disadvantage of drip irrigation is its installation cost, which based on experience in California ranges from US$1500 ha^{-1} to US$2500 ha^{-1}. For drip irrigation to be at least as profitable as the other irrigation methods, more revenue from higher yields and reduced irrigation and cultural costs must occur.

Between 1998 and 2003, experiments in commercial fields on the west side of the San Joaquin Valley evaluated the effect of subsurface drip irrigation on processing tomato under saline, shallow groundwater conditions (Hanson and May, 2004; Hanson et al., 2006a). Subsurface drip irrigation of processing tomato under these conditions was highly profitable compared with sprinkle irrigation. The average profit of the three drip-irrigated fields was $1195 ha^{-1} higher than for sprinkle irrigation. As a result, subsurface drip irrigation of processing tomato has increased considerably in the salt-affected areas.

A key to the profitable subsurface drip irrigation of tomato under saline, shallow groundwater conditions is salinity control in the root zone, which involves leaching salts from the root zone by applying irrigation water in excess of the soil moisture depletion. The leaching fraction, used to quantify leaching adequacy, is defined as the amount of water that drains below the root zone divided by the amount applied.

Leaching fractions are determined in several ways for commercial fields. One approach is to measure the average root zone soil salinity and the salinity of the irrigation water and then use appropriate charts or equations to determine the leaching fraction (Ayers and Westcott, 1985). Under drip irrigation, however, soil salinity, soil water content, and root density all vary around the drip line, and as a result, uncertainty exists in the average root zone salinity and thus, the leaching fraction under drip irrigation.

A second approach commonly used is the water balance method, which calculates the field-wide amount of leaching as the difference between seasonal amounts of applied water and evapotranspiration. The crop evapotranspiration frequently is assumed to equal the potential evapotranspiration (ET_{pot}), calculated using crop coefficients and a reference crop evapotranspiration (Allen et al., 1998).

Field-wide leaching fractions were calculated for the commercial fields of the previously mentioned experiments using the water balance approach. The actual evapotranspiration was determined using canopy growth rates and a calibrated computer evapotranspiration model. These calculations showed little or no field-wide leaching at most of the sites (Table 1), which suggests inadequate salinity control and raises questions about the sustainability of drip irrigation under these saline, shallow groundwater conditions.

Soil salinity measurements in the commercial fields (Fig. 1 and 2), however, clearly showed that substantial leaching occurred near the drip lines because of the wetting patterns under drip irrigation, and that the leaching was highly concentrated near the drip line. It was found that soil salinity near drip lines depended on the depth to the saline groundwater, the electrical conductivity (EC) or salinity of the shallow groundwater (EC_{gw}), the irrigation water salinity (EC_{iw}), and the amount of applied irrigation water (AW). For a water table depth of about 2 m, soil salinity was low and relatively uniform throughout the soil profile even though EC_{gw} ranged from 7.9 to 11.1 dS m^{-1} (Fig. 1A). Irrigation water salinity was 0.3 dS m^{-1}, which reflected the salinity of the surface irrigation water commonly used in the salt-affected area. For water table depths of 0.6 to 1 m, soil salinity was the smallest near the drip line, but increased considerably with distance and depth from the drip lines for a condition where EC_{iw} = 0.3 dS m^{-1} and EC_{gw} = 5 to 7 dS m^{-1} (Fig. 1B). The observed high salinity levels in the soil profiles were due to upward flow of the shallow saline groundwater. An EC_{iw} = 1.1 dS m^{-1} increased soil salinity near the drip line (Fig. 1C), and the volume of leached soil near the drip line increased as the amount of applied irrigation water increased for a water table depth ranging from 0.46 to 0.6 m (EC_{iw} = 0.52 dS m^{-1}, EC_{gw} = 8 to 11 dS m^{-1}; Fig. 2). Because of the shallow groundwater depth, the irrigation water displaced the shallow groundwater directly beneath the drip line. The experiments in the commercial fields also showed that a seasonal water application about equal to the seasonal crop evapotranspiration provided sufficient leaching near the drip lines, yet minimized water table fluctuations due to irrigation.

The soil salinity data from the commercial fields indicated that the water balance approach is not appropriate for drip irrigation and that estimating actual leaching fractions with drip irrigation under saline shallow groundwater conditions using the traditional approaches may be difficult if not impossible because of the spatial variability of soil salinity under these conditions. Therefore, we conducted a numerical modeling study using the HYDRUS-2D computer simulation model to evaluate leaching with subsurface drip irrigation under saline, shallow groundwater conditions for different amounts of applied water, water

Table 1. Seasonal applied water and evapotranspiration, and field-wide leaching fractions calculated from a water balance for the four commercial sites, identified by the designations of BR, DI, DE, and BR2.

Year	Seasonal applied water	Seasonal evapotranspiration	Leaching fraction
	cm		%
	BR		
1999	41	52	0
2000	43	54	0
2001	52	58	0
	DI		
1999	56	64	0
2000	74	64	13.1
2001	58	68	0
	DE		
2000	73	61	13.6
2001	56	59	0
	BR2		
2002	59	62	0

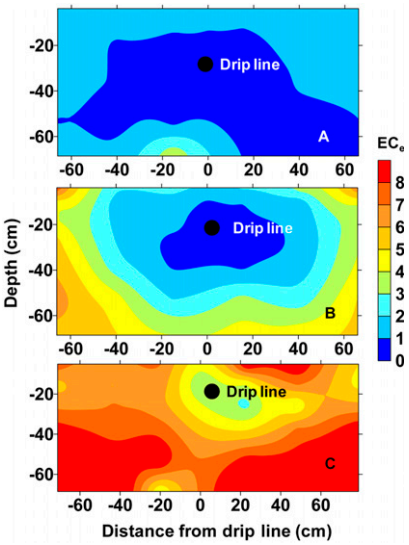

Fig. 1. Measured distributions of soil salinity around drip lines for (A) average water table depth = 2 m, irrigation water electrical conductivity (EC_{iw}) = 0.3 dS m^{-1}, and groundwater electrical conductivity (EC_{gw}) = 8 to 11 dS m^{-1}; (B) water table depth between 0.61 and 1 m, EC_{iw} = 0.3 dS m^{-1}, and EC_{gw} = 5 to 7 dS m^{-1}; and (C) water table depth between 0.61 and 1 m, EC_{iw} = 1.1 dS m^{-1}, and EC_{gw} = 9 to 16 dS m^{-1}. The dots are the drip line locations. Values are EC of saturated extracts (dS m^{-1}).

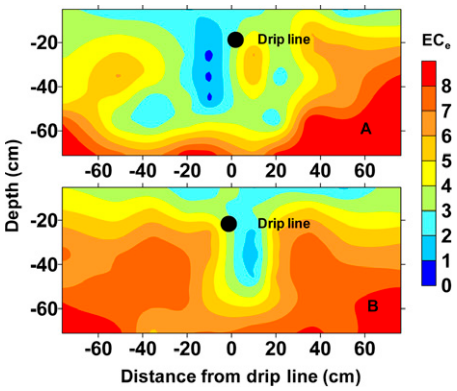

Fig. 2. Effect of amount of applied irrigation water on the measured distributions of soil salinity around the drip line for (A) 589 mm of applied water (about equal to the seasonal evapotranspiration of processing tomato), and (B) 397 mm of applied water. Irrigation water electrical conductivity (EC) = 0.52 dS m^{-1} and groundwater EC = 8 to 11 dS m^{-1}. The dots are the drip line locations. Values are EC of saturated extracts (dS m^{-1}).

table depths, and irrigation water salinity and to estimate leaching fractions with subsurface drip irrigation under these conditions. The HYDRUS-2D model has been previously used in studies of water and chemical movement under drip irrigation using the identical model domains and boundary conditions that were used in this study (Gärdenäs et al., 2005; Hanson et al., 2006b).

This research specifically addresses the threat of soil salinization in the western San Joaquin Valley, where traditional approaches to salinity and water table control through installation of subsurface drainage systems and drainage water disposal facilities are not feasible. We believe that our study provides new insights on the behavior of drip irrigation under saline, shallow groundwater conditions.

Materials and Methods

Soil water and soil water salinity distributions around the drip line were modeled with the computer simulation model HYDRUS-2D (Šimůnek et al., 1999). This software package can simulate the transient two-dimensional movement of water and nutrients in soils. In addition, the model allows specification of root water uptake, which affects the spatial distribution of water and soil water salinity between irrigation cycles. For a detailed description of the application of HYDRUS-2D, we refer to the studies by Gärdenäs et al. (2005) and Hanson et al. (2006b). The database of HYDRUS includes parameter values that specify soil hydraulic properties of the loam soil type of this simulation study, which was typical of the soils in the previously discussed commercial fields. The van Genuchten–Mualem model (van Genuchten, 1980) described the soil water retention and unsaturated hydraulic conductivity relationships with the following hydraulic parameters: saturated hydraulic conductivity (K_s) = 24.96 cm d^{-1}, residual soil water content (θ_r) = 0.078, saturation soil water content (θ_s) = 0.43, n = 1.56, α = 0.036 cm, and l = 0.5. Longitudinal dispersivity was considered to be 5 cm and molecular diffusion was neglected. Simulation output included the spatial and temporal variations of soil water content, soil water salinity, soil water pressure head, and the total water and salt mass in the simulated soil profile.

The simulated subsurface drip irrigation system design characteristics were typical of the drip systems used for processing tomato, with a drip line depth of 20 cm and an emitter spacing of 30 cm. The simulated model domain was 100 cm deep and 75 cm wide (one half of the bed spacing used for tomato production; Fig. 3), representing the dominant presence of roots based on field observations. The transport domain was discretized into 5000 finite elements with very fine grid around the dripper (0.2 cm) and gradually increasing elements farther from the drip (up to 4 cm). The simulations assumed zero water flux boundary conditions along the vertical sides of the soil domain, a zero pressure groundwater table at either the 50- or 100-cm depth with a hydrostatic pressure head distribution below and above the groundwater table, and an atmospheric boundary condition at the top of the domain, where ET = ET_{pot} for unstressed root water uptake conditions. It was assumed that the crop was fully mature with a canopy coverage (percentage of soil shaded by the canopy at midday) of 90% and that ET represents transpiration only (i.e., evaporation was assumed to be zero). Drip irrigation was represented using the system-independent time-variable flux boundary condition along the dripper circumference. The radius of the dripper was assumed to be 1.1 cm and the irrigation discharge 11.975 L d^{-1}. The drip irrigation was simulated assuming an infinite line source, which was shown previously by Skaggs et al. (2004) to be a good representation of this drip irrigation system. The line-source approach also was used in the previously mentioned studies on water and chemical movement.

The zero pressure water table resulted in a constant pressure boundary at the bottom of the domain. This boundary condition allowed drainage water to flow out of the domain without raising the water table, assuming that sufficient natural groundwater drainage was occurring. This approach provided an estimate of the potential leaching fraction below the drip line. A similar response of little or no change in the water table depth due to irrigation was found in the previously mentioned drip irrigation experiments in the commercial fields, except when overirrigation occurred, suggesting adequate natural drainage at these locations.

Simulations were conducted during a 42-d period for water table depths of 50 and100 cm, EC_{iw} of 0.3, 1.0, and 2.0 dS m^{-1}, and AW amounts equal to 80, 100, and 115% of the potential daily evapotranspiration rate (ET_{pot} = 7.5 mm d^{-1}). For the EC_{iw} = 0.3 dS m^{-1} scenario, we included a water application of 60% of ET_{pot}. These EC_{iw} values reflect the range found in the commercial fields. Surface water with EC_{iw} values generally between 0.3 and 0.5 dS m^{-1} is the most common source of irrigation water in the salt-affected areas of the valley, hence our focus was on the smaller irrigation water salinity. In some cases, groundwater may be used with EC_{iw} values generally between 1 and 2 dS m^{-1}. The EC_{gw} was assumed to be 8 dS m^{-1} for the 100-cm water table depth and 10 dS m^{-1} for the 50-cm depth, based on EC measurements of the shallow groundwater in the commercial fields. Selected irrigation frequencies were twice per week and daily for the 100- and 50-cm water table depth scenarios, respectively. These parameters of water table depth, groundwater and irrigation water salinity, and applied water were selected because they are representative of the commercial fields. Spatial distribution of salinity in the transport domain was simulated using the convection–dispersion equation for a nonreactive tracer. Such simulations cannot account for complex processes such as precipitation or dissolution of solid phases (e.g., gypsum or calcite) or cation exchange.

Hydrostatic pressure head conditions were assumed for the initial conditions. Initial soil water salinities were based on field measurements made in the spring, before drip irrigation, and

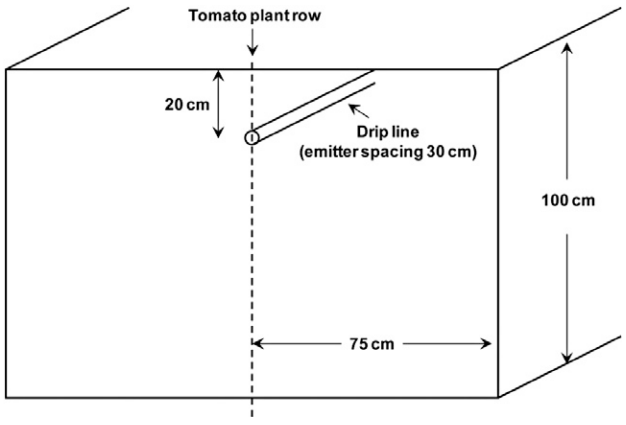

FIG. 3. Model domain for the subsurface drip irrigation system.

were determined from EC measurements of the saturated soil extract (EC_e), the volumetric soil water content (θ), and the saturation percentage (SP) of collected soil samples. The SP was 53 and 62% for the 100- and 50-cm water table depths, respectively. These values were measured in the commercial fields for similar water table depths. The initial soil water salinity (EC_{sw}) was calculated from:

$$EC_{sw} = (EC_e)(SP)/\theta \quad [1]$$

These initial conditions reflect the effects of rainfall, sprinkle irrigation (preplant and stand establishment), evaporation, and upward flow from the shallow groundwater on soil salinity before the start of drip irrigation.

The root distribution in Fig. 2 was described using the model of Vrugt et al. (2001), with most roots extending 35 cm laterally and 30 or 40 cm vertically for scenarios with the groundwater table 50 and 100 cm deep, respectively (Fig. 4). The following parameters of the Vrugt et al. (2001) model were used: Z_m = 40 cm, X_m = 35 cm, x^* = 5 cm, p_x = 1, z^* = 25 cm, p_z = 2. The reducing effects of both soil water pressure head (Feddes et al., 1978) and osmotic head on root water uptake were included, assuming that their effects were multiplicative. The following parameters of the Feddes et al. (1978) model were used: h_0 = −1, h_{opt} = −2, $h_{2,high}$ = −800, $h_{2,low}$ = −1500, h_3 = −8000 cm; $r_{2,high}$ = 0.5 cm d^{-1}, and $r_{2,low}$ = 0.1 cm d^{-1}. The threshold model (Maas, 1990) was used to described the osmotic effects using a threshold EC_e = 2.5 dS m^{-1} and a slope of 9.9%.

These root distributions were used for all scenarios because little information is available on the effect of a given scenario on root distribution, although in reality the distributions may differ with the amount of AW, the EC_{iw}, and the water table depth. Even though the root distributions were constant, the spatial distribution of the root water uptake varied between scenarios because of the effects of both pressure head and osmotic potential on root water uptake.

Observation nodes were selected at specific locations in the domain to monitor levels of soil water salinity and content with time, as simulated by the HYDRUS model. These nodes were located at distances of 0, 10, 20, and 30 cm from the center of the tomato bed and at depths of 0, 10, 20, 35, and 60 cm, for a total of 20 nodes.

Results

Soil Water Content Patterns

Because of the hydrostatic initial condition, the initial soil water content (t = 0) increased with increasing depth for both the 100- and 50-cm water table depth scenarios (Fig. 5). At the end of the first drip irrigation (t = 1 d) of the 100-cm water table scenario, soil water content increased substantially near the drip line, extending to near the soil surface and about 30 cm laterally at the depth of the drip line (top row, Fig. 5). Water content also increased down to about 50 cm deep directly below the drip line. Just before the next irrigation (t = 3.5 d), substantial drying occurred around the drip line because of root water uptake. Little root water uptake occurred beyond about 20 cm from the drip line because of the low root density. Similar wetting and drying cycles occurred throughout the total simulation period of 42 d.

For the 50-cm-deep water table scenario (bottom row, Fig. 5), water content was at saturation below the 50-cm depth. Just after irrigation (t = 0.28 d), soil water content was maximum near the drip line. Before the next irrigation (t = 1 d), water content decreased near the drip line, with the lowest water content near the surface. Soil water content patterns throughout the simulation period (t = 40.28 d) were similar.

Soil Water Salinity

The initial EC_e values varied between 5.5 dS m^{-1} (top 0.15 m of soil) and 8.7 dS m^{-1} (water table) for the 100-cm water table scenario (data not shown). Converting the EC_e data to soil water EC (EC_{sw}) resulted in corresponding initial EC_{sw} values varying from 7.1 dS m^{-1} near the soil surface to 8.0 dS m^{-1} (EC of the shallow groundwater) at the water table. Thus, the initial EC_{sw} values were nearly constant with depth (top row, Fig. 6).

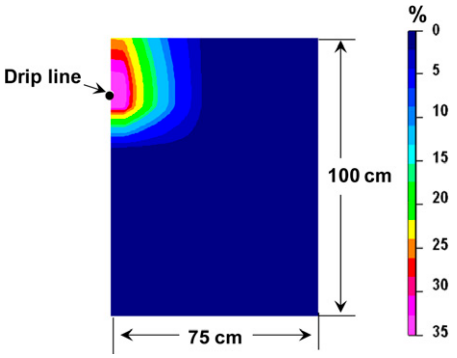

FIG. 4. Root distribution used for the HYDRUS-2D simulations for the 100-cm water table depth scenarios. Units on the scale are the percentages of the total roots.

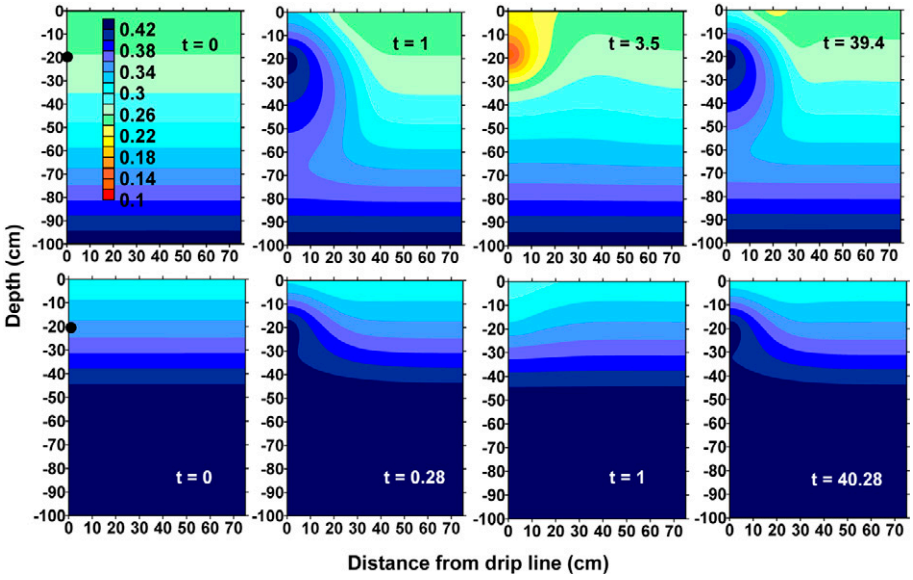

FIG. 5. Simulated distributions of the volumetric soil water content in the domain for both the 100-cm water table depth scenario (upper contour plots) and the 50-cm water table depth scenario (lower contour plots). Values in the contour plots are the times (days) during the simulation period. The black dots are the drip line locations. Water application = 100% and irrigation water electrical conductivity = 0.3 dS m^{-1}.

After the first irrigation of the 100-cm water table depth scenario (t = 1, top row, Fig. 6), considerable localized leaching occurred near the drip line, with EC_{sw} values smaller than 1 dS m^{-1} immediately adjacent to the drip line. Soil salinity increased with distance from the emitter and with soil depth. Salt leaching occurred to about the 55-cm soil depth and to about 25 cm laterally away from the drip line. Before the next irrigation, EC_{sw} increased slightly near the drip line because of root water uptake. In addition to a downward displacement of a low salt zone, a zone of higher soil salinity formed near the soil surface, extending to about 25 cm from the center of the soil bed. As time progressed (t = 39.4 d), leaching around the drip line increased, with most of the leaching below the drip line (Fig. 6). Simultaneously, the higher salt zone near the soil surface increased in size, with salt concentrations higher than those of the initial soil conditions. No leaching occurred beyond about 50 cm from the drip line.

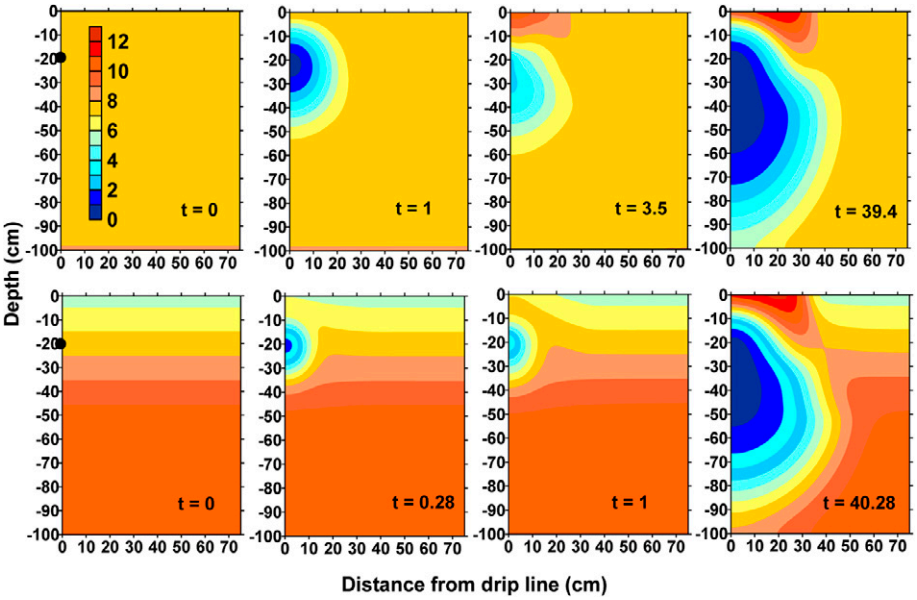

FIG. 6. Simulated distributions of soil water salinity for the 100-cm water table depth scenario (upper contour plots) and the 50-cm water table depth scenario (lower contour plots). Values in the contour plots are the times (days) during the simulation period. The black dots are the drip line locations. Applied water = 100% and irrigation water electrical conductivity = 0.3 dS m^{-1}.

For the 50-cm water table depth scenario (bottom row, Fig. 6), the initial EC_{sw} values increased from about 5.5 dS m^{-1} near the soil surface to about 10 dS m^{-1} (EC of the groundwater) at the water table depth. At the end of the first irrigation (t = 0.28, bottom row, Fig. 6), localized leaching occurred around the drip line to about 10 cm horizontally from the drip line. The volume of leached soil was smaller than that for the deeper water table scenario at the end of the first irrigation due to the smaller amounts of water applied during the daily irrigations. Just before the next irrigation (t = 1, bottom row, Fig. 6) a slight increase in EC_{sw} occurred near the drip line. As time progressed, the volume of leached soil increased, with applied water displacing the shallow groundwater at depths below 50 cm. Much of the leaching occurred at depths below the drip line (t = 40.28, bottom row, Fig. 6). Some leaching occurred above the drip line, although salt accumulated near the soil surface. The zone of accumulated salt extended nearly 30 cm from the center of the bed.

Increasing the amount of AW increased the leached zone for the 100-cm water table depth scenarios (top row, Fig. 7). Even for water applications of 60% of ET_{pot} (severe deficit irrigation), however, some leaching occurred near the drip line. Increasing the amount of AW slightly affected the salinity pattern above the drip line, but greatly increased the leached zone below the drip line. Similar behavior occurred for the 50-cm water table depth scenarios (data not shown). This behavior of both scenarios was similar to that of the field data (Fig. 2).

Increasing the EC_{iw} increased EC_{sw} near the drip line for the 100-cm scenario (AW = 100%), as would be expected (bottom row, Fig. 7). Values of EC_{sw} near the drip line were <1 dS m^{-1} for the low-salt irrigation water (EC_{iw} = 0.3 dS m^{-1}), but increased to values >3 dS m^{-1} for EC_{iw} = 2 dS m^{-1}. The soil volume of high salinity near the soil surface also increased as the EC_{iw} increased, as would be expected. Similar behavior occurred for the 50-cm water table depth scenarios (data not shown).

A cyclic behavior in EC_{sw} with time was found at most observation nodes for the 100-cm water table depth scenario,

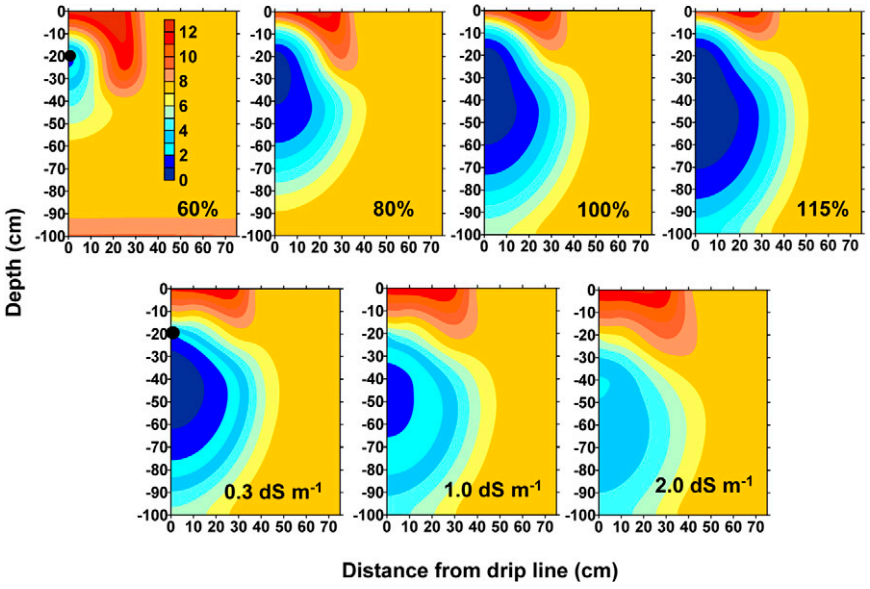

FIG. 7. Simulated distributions of soil water salinity (EC_{sw}) at the end of the simulation period for (top row) amounts of applied water equal to 60, 80, 100, and 115% of the potential evapotranspiration (irrigation water electrical conductivity [EC_{iw}] = 0.3 dS m^{-1}); and (bottom row) distributions of EC_{sw} for EC_{iw} = 0.3 dS m^{-1}, 1.0 dS m^{-1}, and 2.0 dS m^{-1} (applied water = 100%). The black dots are the drip line locations.

reflecting the irrigation and subsequent root water uptake (Fig. 8, A1–D1). Values of EC_{sw} near the surface increased with additional irrigations to values larger than the initial condition. At the 10-cm depth, large fluctuations occurred at all distances, but they decreased in magnitude as distance increased. At 20 cm deep (depth of the drip line), EC_{sw} quickly decreased at the bed center, reflecting the effect of EC_{iw}. The decrease became smaller as distance from the bed center increased. Below the drip line, EC_{sw} decreased with time for all distances to values considerably smaller than the initial condition because of leaching. The rate of decrease was smaller as the distance and depth below the drip line increased.

The cyclic behavior was less pronounced for the 50-cm water table depth scenarios because of the daily irrigations and smaller water applications per irrigation (Fig. 8, A2–D2). Near the soil surface, EC_{sw} increased to levels greater than the initial condition. The rate of soil salinity increase was largest at the bed center, and was more gradual with time as lateral distance increased. At 10 cm deep, EC_{sw} decreased with time except at the 30-cm distance, while at 20 cm deep, EC_{sw} decreased with time at distances near the bed center but increased at distances $\geq$20 cm. Below the drip line depth, EC_{sw} decreased with time regardless of distance from the bed center. These trends were similar for the other water applications and irrigation water salinities. At depths below the drip line, however, final values of EC_{sw} depended on the amount of applied water and EC_{iw}.

Salt Mass

The numerical solution provided the final (t = 42 d) salt mass in the soil domain from mass balance computations computed from salt input by the incoming irrigation water, salt leaching at the bottom of the simulated soil domain, and the initial salt mass. The total salt mass in the profile decreased with time (Table 2 for the 100-cm water table depth) for all scenarios, with the salt decrease proportional to applied irrigation water; however, differences were only minor for the EC_{iw} = 2.0 dS m^{-1} scenario. The mass balance results were similar for the 50-cm water table depth (data not shown).

Above the drip line, the salt mass increased with time (Fig. 9A). For a given EC_{iw}, the increase was the highest for the smallest water application. As expected, the salt mass above the drip line also increased as EC_{iw} increased, although only slight differences in the final total salt mass occurred for the 80, 100, and 110% ET scenarios at EC_{iw} = 2 dS m^{-1}. Similar results were obtained for the 50-cm water table depth scenarios (data not shown). Our simulation results indicated that for deficit water applications, water flow and salt transport into the zone above the drip line was partially driven by capillary forces, causing upward

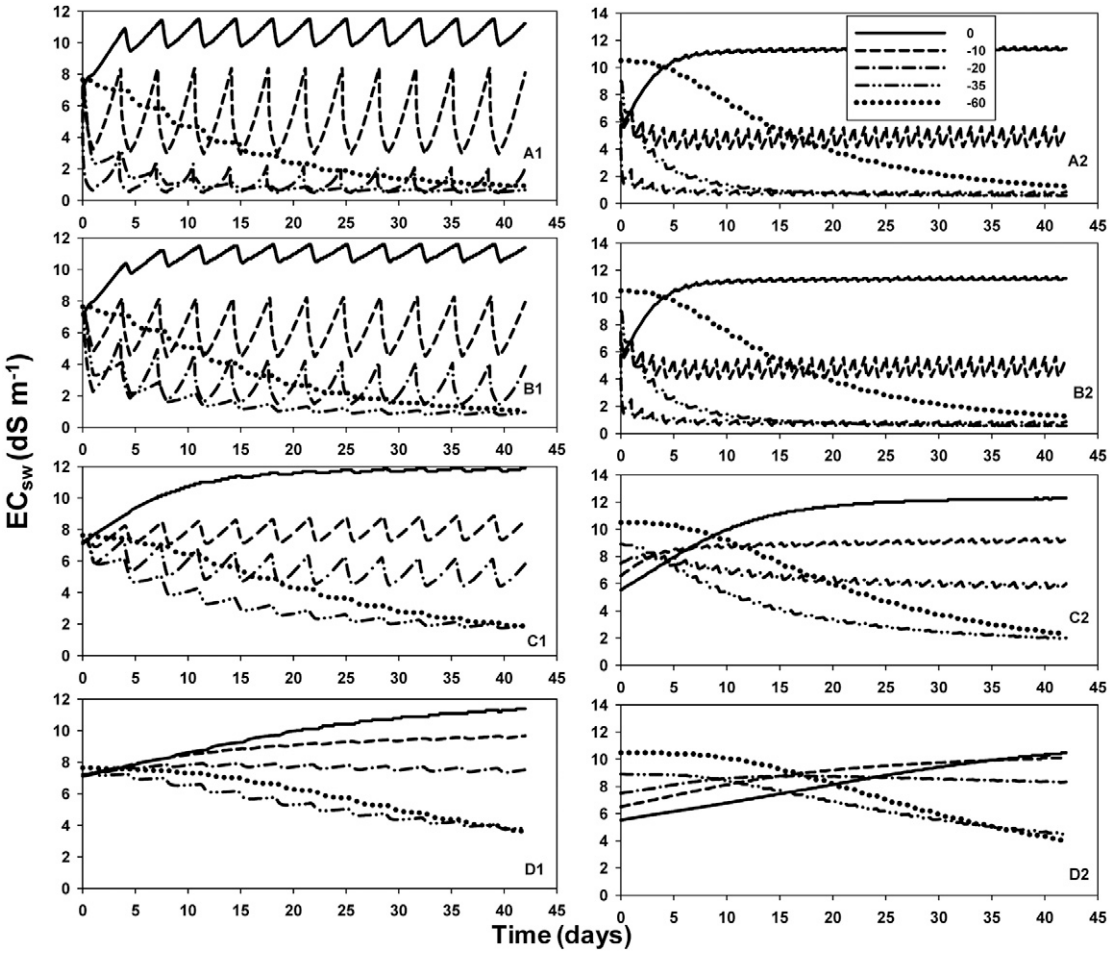

FIG. 8. Soil water salinity (EC_{sw}) data with time at the observation nodes for distances of (A1) 0, (B1) 10, (C1) 20, and (D1) 30 cm from the center of the bed at depths of 0, 10, 20, 35, and 60 cm for the 100-cm water table depth scenario (applied water [AW] = 100%, irrigation water electrical conductivity [EC_{iw}] = 0.3 dS m^{-1}); and for distances of (A2) 0, (B2) 10, (C2) 20, and (D2) 30 cm from the center of the bed at depths of 0, 10, 20, 35, and 60 cm for the 50-cm water table depth scenario (AW = 100%, EC_{iw} = 0.3 dS m^{-1}).

Table 2. Relative salt mass balance for the 100-cm water table depth scenario. Values are expressed as a fraction of the initial mass, which was the same for all scenarios. The added salt is the salt in the irrigation water. The amount of leached salt is the salt that moved across the bottom of the domain.

Applied water	Initial	Added	Leached	Final
%				
		Irrigation water electrical conductivity (EC_{iw}) = 0.3 dS m^{-1}		
60	1	0.02	0.05	0.97
80	1	0.03	0.15	0.88
100	1	0.04	0.26	0.77
115	1	0.05	0.34	0.70
		EC_{iw} = 1.0 dS m^{-1}		
80	1	0.11	0.19	0.91
100	1	0.13	0.30	0.82
115	1	0.15	0.38	0.76
		EC_{iw} = 2.0 dS m^{-1}		
80	1	0.21	0.25	0.95
100	1	0.26	0.37	0.89
115	1	0.30	0.45	0.85

and lateral salt transport, which resulted in higher salt masses about the drip line for the deficit irrigation conditions than for the well-watered conditions.

As expected, the salt mass decreased with time below the drip line (Fig. 9B) because of leaching, thereby decreasing the salt mass as AW increased. This salt decrease, however, was less pronounced as the salinity of the applied water increased. Similar results were obtained for the 50-cm water table depth, although differences between EC_{iw} values for a given amount of applied water were slightly larger than those differences for the 100-cm depth scenario (data not shown).

Water Balance and Leaching

Water uptake by roots showed a strong cyclic effect between irrigations for the 100-cm water table depth scenario (Fig. 10A). Water uptake increased and time fluctuations decreased as AW increased except for AW = 60%. The increase in the root uptake with AW reflects the larger values of soil water content near the drip lines. Root water uptake decreased as the salinity of the irrigation water increased, because of increasing salt stress effects. We note that for no-stress soil conditions, root water uptake must be equal to 7.5 mm d^{-1} (ET_{pot}). The results of the 50-cm water table depth scenarios (Fig. 10B) were similar; however, fluctuations between the daily irrigations were much smaller due to the irrigation frequency. Maximum root water uptake values between irrigations for a given amount of applied water and EC_{iw} were smaller than those of the deeper water table scenarios.

Water uptake increased slightly with time for the first 10 d for AW = 100 and 115%, suggesting that leaching of the root zone increased during that time period. The higher values of AW

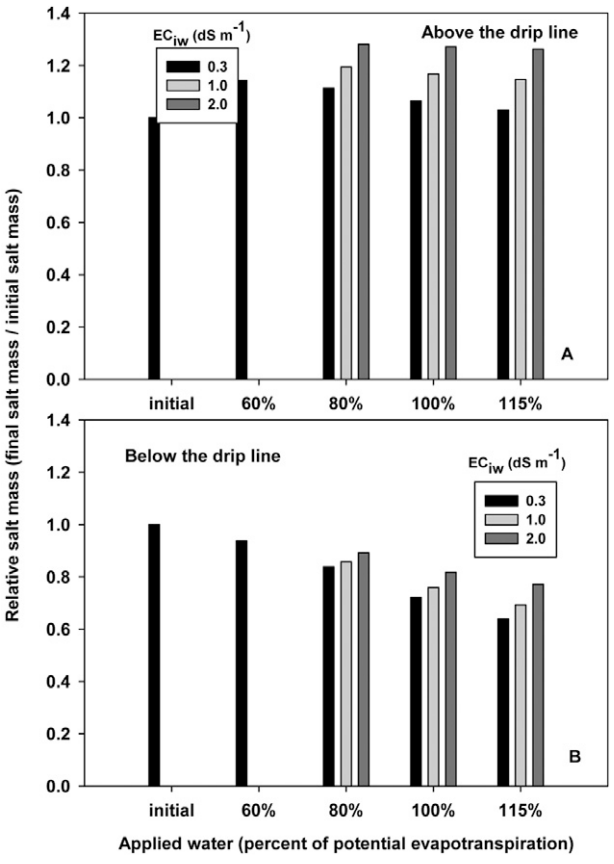

Fig. 9. The initial and final relative salt masses for water applications of 60, 80, 100, and 115% and irrigation water electrical conductivity (EC_{iw}) = 0.3, 1.0, and 2.0 dS m^{-1} for (A) above and (B) below the drip line depth. Values are expressed as a fraction of the initial mass. Data for the 60% water application was determined for EC_{iw} = 0.3 dS m^{-1} only.

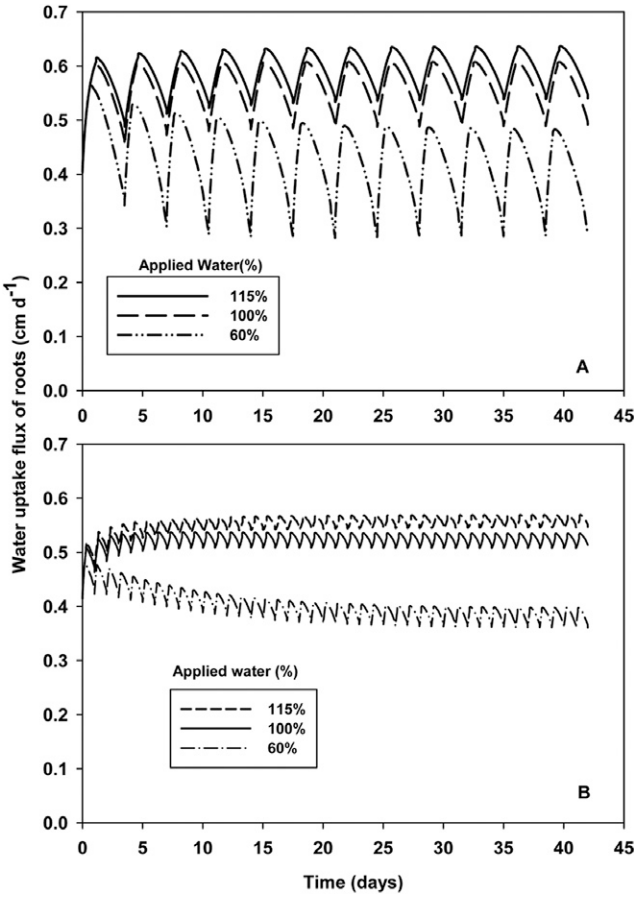

Fig. 10. Water uptake fluxes by roots for (A) 100-cm and (B) 50-cm water table depth scenarios (applied water = 60, 100, and 115%; irrigation water electrical conductivity = 0.3 dS m^{-1}). Positive values indicate water flow out of the domain; negative values indicate water flow into the domain.

= 115% may reflect more leaching for that scenario, although higher soil water contents probably were also a factor. For AW = 60%, water uptake decreased with time during the first 15 d, which may reflected limited leaching in the root zone along with smaller soil water contents.

The water flux at the domain bottom (i.e., leaching) showed a cyclic behavior caused by the periodic irrigations (Fig. 11A for the 100-cm water table depth scenario), with flux values increasing as the AW increased. Occasionally, water flux was negative for AW = 60%, indicating upward water flow from the fixed groundwater table. As the salinity of the irrigation water increased, the leaching amount increased because of reduced water uptake (data not shown). A trend of decreasing water flux occurred for the first 10 to 15 d, but thereafter, little trend was found.

A cyclic water flux behavior was also found for the 50-cm-depth scenarios (data not shown) although water flux values were considerably higher than for the 100-cm water table depth scenarios. Moreover, upward water and salt fluxes were significantly higher than for the 100-cm water table depth scenarios.

As expected, salt transport across the bottom of the soil domain was cyclic as well (Fig. 11B), with larger salt fluxes as AW increased. Solute fluxes decreased with time, with the largest decrease for AW = 115%. This behavior reflects a decrease in the amount of salt transported from the domain with time as the localized reclamation of the soil profile progressed.

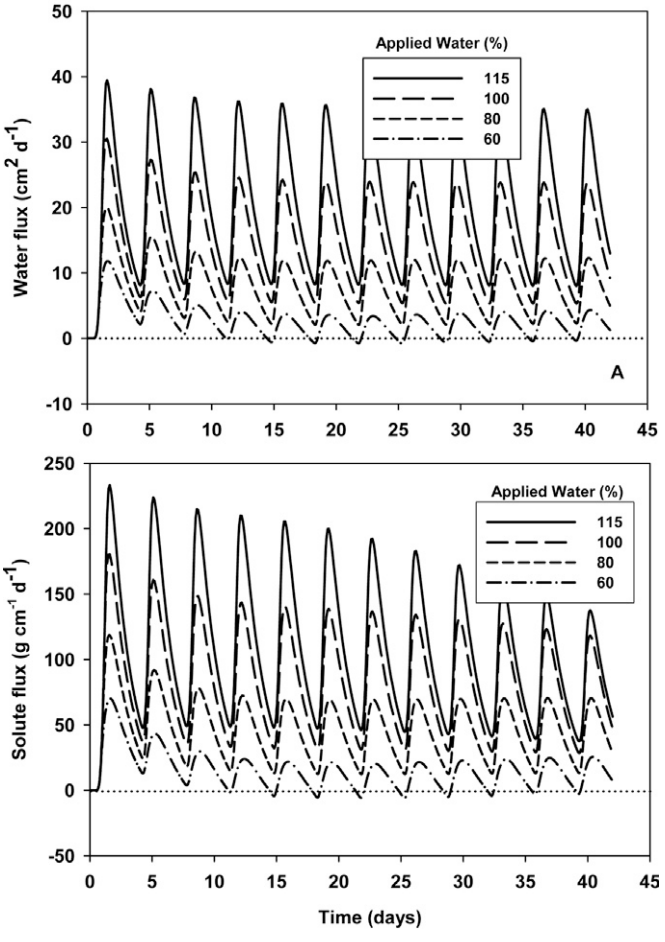

FIG. 11. Fluxes at the bottom of the domain of (A) water and (B) solute for different water applications (irrigation water electrical conductivity = 0.3 dS m^{-1}). Positive values indicate water flow out of the domain; negative values indicate water flow into the domain.

Cumulative amounts of AW, root water uptake, and leaching at the bottom of the soil domain are presented in Table 3. Seasonal root water uptake decreased as AW decreased, suggesting that shallow groundwater contribution to the crop's water demand is limited by both the soil's hydraulic conductivity and assumed root zone distribution. As a result, we expect crop yield to decrease as well. Experimental data obtained in the commercial fields (Hanson and May, 2004; Hanson et al., 2006a) confirmed a linear relationship between tomato yield and applied water, with yield decreasing as AW decreased.

We define the localized leaching fraction (LLF) as the actual leaching fraction representative of the local irrigated root domain near the drip line. The LLF values ranged from 7.7 to 30.9% as AW increased from 60 to 115% for the 100-cm water table depth scenario (EC_{iw} = 0.3 dS m^{-1}) and from 11.3 to 36.1% for the 50-cm water table depth scenario (EC_{iw} = 0.3 dS m^{-1}) (Table 3). As the salinity of the irrigation water increased, LLF values increased due to reduced root water uptake for the higher salinity levels (Table 3). The LLF values were generally higher for the 50-cm water table depth scenarios due to reduced root water uptake compared with the deeper water table scenarios (Table 3). Similar LLF values were obtained using a water balance approach with the drainage amount equal to the difference between cumulative applied water and root uptake, as calculated by HYDRUS-2D.

TABLE 3. Amount of applied water, root uptake, drainage, and localized leaching fraction (expressed as a percentage) for different amounts of applied water (expressed as a percentage of the potential crop evapotranspiration), different water table depths, and different irrigation water electrical conductivities (EC_{iw}).

Applied water	Applied water	Root uptake	Drainage	Leaching fraction
%	cm^2			%
	Water table depth = 100 cm, EC_{iw} = 0.3 dS m^{-1}			
60	1410	1350	109	7.7
80	1890	1580	328	17.3
100	2360	1760	600	24.5
115	2710	1850	837	30.9
	Water table depth = 100 cm, EC_{iw} = 1.0 dS m^{-1}			
80	1890	1440	431	22.8
100	2360	1610	719	30.4
115	2710	1700	962	35.4
	Water table depth = 100 cm, EC_{iw} = 2.0 dS m^{-1}			
80	1890	1260	585	30.9
100	2360	1390	899	38.1
115	2710	1480	1150	42.4
	Water table depth = 50 cm, EC_{iw} = 0.3 dS m^{-1}			
60	1414	1263	161	11.3
80	1886	1474	418	22.2
100	2357	1642	724	30.7
115	2711	1738	979	36.1
	Water table depth = 50 cm, EC_{iw} = 1.0 dS m^{-1}			
80	1886	1360	531	28.1
100	2357	1508	853	36.2
115	2711	1597	1116	41.2
	Water table depth = 50 cm, EC_{iw} = 2.0 dS m^{-1}			
80	1886	1197	690	36.6
100	2357	1326	1029	43.7
115	2711	1407	1301	48.0

Discussion

Our results showed that the water balance approach to determining leaching fractions is inappropriate for drip irrigation. Both the simulation and experimental data by Hanson and May (2004) and Hanson et al. (2006a) demonstrated that considerable localized leaching occurs near the drip lines, including under deficit irrigation conditions (AW < ET_{pot}). We showed that for water applications of 100% or smaller (EC_{iw} = 0.3 dS m^{-1}), the LLFs ranged from 7.7 to 11.3% for AW = 60%, 17.3 to 22.2% for AW = 80%, and 24.5 to 30.7% for a 100% water application. Localized leaching fractions increased as the salinity of the irrigation water increased because of the corresponding reduction of the root water uptake. When using the conventional definition of LF, as generally applicable to low-frequency sprinkle and surface irrigation methods, computations of LF for water applications equal to 100% of ET_{pot} or smaller will result in zero leaching values using the water balance approach.

The spatially variable soil wetting patterns that occur under drip irrigation lead to localized leaching below the drip line, in spite of applying irrigation water at rates <ET_{pot}. The localized leaching is concentrated near the drip line, as indicated by the EC_{sw} patterns (Fig. 6), thus resulting in a potential for a greater reduction of salts in the root zone than would occur for sprinkle or surface irrigation methods for a given AW amount.

Our simulation results also showed salt accumulation above the drip line, near the soil surface, potentially negatively affecting crop establishment. To prevent this, periodic leaching is needed by either seasonal rainfall or a preplant sprinkle irrigation, moving the accumulated salt below the drip line and away from the rooting zone.

The simulation results also showed that larger water applications per irrigation event at a relatively low irrigation frequency reclaim the soil faster than smaller applications at a higher frequency (Fig. 6). Thus, several large applications of about 24 h each should be applied for new drip systems installed in a saline soil to quickly reclaim the soil near the drip line.

Conclusions

This analysis using numerical simulations of various subsurface drip irrigation scenarios included two shallow groundwater table depths, a range of irrigation water and groundwater salinities, and various water application values. The studies provided valuable insights into salt leaching processes with subsurface drip irrigation under saline, shallow groundwater conditions, supported by experimental data for similar soil and irrigation water conditions. The main conclusions derived were that (i) salt reclamation near the drip lines occurs quite rapidly after the onset of irrigation; (ii) large applications per irrigation event reclaim the soil more quickly than do smaller applications at a higher frequency; (iii) the size of the leached soil region near the drip line is controlled by the amount of applied water; (iv) soil salinity of the leached soil zone increases as the salinity of the irrigation water increases; (v) localized salt leaching around the drip line occurs even for deficit irrigation conditions; and (vi) the conventional method for calculating leaching fractions, used for sprinkle and surface irrigation methods, is inappropriate for drip irrigation.

A common assumption is that an amount of applied water equal to 100% ET_{pot} results in an irrigation efficiency of 100% for drip irrigation, and that little drainage below the root zone occurs. These results show that assumption is not true. Because of the spatially varying soil water wetting around drip lines, the irrigation efficiency, defined as the ratio of the cumulative root water uptake to the applied water, was 74.6 and 69.7% for the 100- and 50-cm water table scenarios, respectively. Very high irrigation efficiencies occurred only under severe deficit irrigation conditions. Because of high frequency irrigation, however, the volume of drainage per irrigation is small and the drainage is distributed evenly across the irrigation season. As a result of this behavior, the natural subsurface drainage in the previously discussed commercial fields appeared to be sufficient to prevent groundwater intrusion into the root zone.

References

Allen, R.G., L.S. Pereira, D. Raes, and M. Smith. 1998. Crop evapotranspiration. FAO Irrig. Drain. Pap. 56. FAO, Rome.

Ayers, R.S., and D.W. Westcott. 1985. Water quality for agriculture. FAO Irrig. Drain. Pap. 29. Rev. 1. FAO, Rome.

California Department of Water Resources. 2005. Agricultural drainage reduction and reuse program. Available at www.owue.water.ca.gov/agdrain/index.cfm (verified 18 Feb. 2008). California Dep. of Water Resources, Sacramento.

Feddes, R.A., P.J. Kowalik, and H. Zaradny. 1978. Simulation of field water use and crop yield. John Wiley & Sons, New York.

Gärdenäs, A., J.W. Hopmans, B.R. Hanson, and J. Šimůnek. 2005. Two-dimensional modeling of nitrate leaching for different fertigation scenarios under micro-irrigation. Agric. Water Manage. 74:219–242.

Hanson, B.R., and J.E. Ayars. 2002. Strategies for reducing subsurface drainage in irrigated agriculture through improved irrigation. Irrig. Drain. Syst. 16:261–277.

Hanson, B.R., R.B. Hutmacher, and D.M. May. 2006a. Drip irrigation of tomato and cotton under shallow saline ground water conditions. Irrig. Drain. Syst. 20:155–175.

Hanson, B.R., and D.M. May. 2004. Effect of subsurface drip irrigation on processing tomato yield, water table depth, soil salinity, and profitability. Agric. Water Manage. 68:1–17.

Hanson, B.R., J. Šimůnek, and J.W. Hopmans. 2006b. Numerical modeling of urea–ammonium-nitrate fertigation under microirrigation. Agric. Water Manage. 86:102–113.

Maas, E.V. 1990. Crop salt tolerance. p. 262–304. *In* K.K. Tanji (ed.) Agricultural salinity assessment and management. ASCE Manuals and Rep. on Eng. Practice 71. Am. Soc. Civil Eng., New York.

Schoups, G., J.W. Hopmans, C.A. Young, J.A. Vrugt, W.W. Wallender, K.K. Tanji, and S. Panday. 2005. Sustainability of irrigated agriculture in the San Joaquin Valley, California. Proc. Natl. Acad. Sci. 102:15352–15356.

Šimůnek, J., M. Šejna, and M.Th. van Genuchten. 1999. The HYDRUS-2D software package for simulating two-dimensional movement of water, heat, and multiple solutes in variable saturated media. Version 2.0. IGWMC-TPS-53. Int. Ground Water Modeling Center, Colorado School of Mines, Golden.

Skaggs, T.H., T.J. Trout, J. Šimůnek, and P.J. Shouse. 2004. Comparison of HYDRUS-2D simulations of drip irrigation with experimental observations. J. Irrig. Drain. Eng. 130:304–310.

van Genuchten, M.Th. 1980. A closed-form equation for predicting the hydraulic conductivity of unsaturated soils. Soil Sci. Soc. Am. J. 44:892–898.

Vrugt, J.A., M.T. van Wijk, J.W. Hopmans, and J. Šimůnek. 2001. One-, two-, and three-dimensional root water uptake functions for transient modeling. Water Resour. Res. 37:2457–2470.